Expanded Online Methods

Pressure Overload Model and

Induction of pressure overload in 12-week-old male mice by thoracic aorta constriction (TAC) has been previously described. [1] In brief, after anesthetization and artificial ventilation, the transverse aorta of mice was constricted with the 7-0 nylon suture by ligating the aorta together with a blunted 27-gauge needle, which was pulled out later. Hemodynamic parameters were measured by a 1.4 F Millar Micro-Tip Catheter Pressure Transducer (Millar Instruments, Inc.) inserted from the right carotid artery into aorta and LV. The transducer was connected to a Mac Lab system (AD Instruments) and the systolic blood pressure (BP) and LV end-diastolic pressure (LVEDP) were recorded.

Isolation of Adult Cardiomyocytes and Intracellular Ca^{2+} Measurement

Adult cardiomyocytes were isolated from mice by Langendorff perfusion method and intracellular Ca^{2+} concentration was measured as previously described. [2] Briefly, dissected hearts were rapidly attached to a Langendorff perfusion system, perfused with Ca^{2+}-free solution and digested with type II collagenase, protease and BDM in 100 mmol/L Ca^{2+} solution at 37 °C for 8-12 min. Then, the hearts were washed and LV was excised, minced and shaked in 100 mmol/L Ca^{2+} solution. Cell suspension was filtered and isolated myocytes were kept in 1 mmol/L Ca^{2+} solution at room temperature (RT). Intracellular Ca^{2+} concentration was measured as previously described. [2] In briefly, isolated myocytes were incubated with 3-4 μmol/L fluo-3 AM in HEPES solution for 30 min at RT. After washed by dye-free HEPES solution for more than 15 min, the cells were excited by UV light of 485 nm, and the emission of 530 nm was collected. Measurements were performed at RT within 6 hours after the isolation. The intracellular Ca^{2+} transients were electrically activated at 0.25 Hz, stabilized within 2 min, and then 10 mmol/L caffeine was rapidly applied to the cardiomyocytes just after the pacing was turned off. [2]

Cardiomyocyte Hypertrophy and Extent of Fibrosis in LV Tissues

Heart sections were stained with hematoxylin and eosin (H-E) and cardiomyocyte hypertrophy was evaluated by measuring the cross section area of cardiomyocytes in randomly selected 10 points per LV section and 100 myocytes was calculated for one point. The value was expressed as the area of per 100 cardiomyocytes. The extent of LV fibrosis was measured in 8 fields randomly selected from a section by calculating the relative ratio of van Gieson-stained fibrosis area. [1, 3]

Angiogenesis, Apoptosis and Autophagy in LV Section

The density of capillaries in LV section was examined by CD31 immunostaining (PharMingen), and the number of CD31-positive microvessels per 100 cells was calculated. [2] Apoptosis of cardiomyocytes was detected *in situ* by terminal deoxyribonucleotide transferase-mediated dUTP nick-end labeling (TUNEL) kit (TaKaRa Biomedicals) in paraffin-embedded heart tissue sections. [1] Autophagy of cardiomyocytes was evaluated by LC3b immunostaining using an anti–LC3b antibody (Santa Cruz Biotechnology Inc.) on paraffin sections. Co-staining of apoptosis and autophagy in LV section were performed by staining against a cardiomyocyte-specific antigen, α-MHC (Santa Cruz Biotechnology Inc.).

Isolation and Culture of Adult Mouse Cardiac Fibroblasts

LV tissues from adult mice with sham or TAC for 4 weeks were minced and digested in DMEM containing 0.05% Bovine Serum Albumin (BSA), 1000U/mL Collagenase 2 (Worthington Biochemical Corporation, Lakewood, NJ, USA) and 0.003% trypsin at 37°C

with continuous shaking for 90 min. [4] The dissociated cells were plated for 1 hour to allow fibroblasts to adhere. Following removal of non-adherent cells, cardiac fibroblasts were cultured to confluence in DMEM containing 2.5% FBS. [4] Experiments were performed on the second passage cells plated at a density of ~200 cells per mm^2. The culture medium was changed to serum-free DMEM at 48 hours before use.

[^{3}H]Thymidine Incorporation

DNA synthesis in cardiac fibroblasts was assessed by measuring [^{3}H]thymidine incorporation into the cells. [5] In brief, cultured cardiac fibroblasts were serum-deprived for 48 hours. [^{3}H]thymidine (1.25 μCi/mL) was added 2 hours before the harvest. Plates were then placed on ice, quickly washed three times with 1 mL of ice-cold PBS, incubated 10 min with 1 mL of 10% trichloroacetic acid, and washed twice with 1 mL of 10% trichloroacetic acid and three times with 1 mL of 95% ethanol. Precipitates were solubilized for 1.5 hours in 800 μL of 0.2N NaOH and neutralized, and radioactivity was measured by liquid scintillation spectroscopy.

Western Blotting

Total protein (100 μg) of the LV tissue was size fractionated by SDS-polyacrylamide gel electrophoresis (SDS-PAGE) and transferred to Immobilon-P membranes (Millipore). Antibodies used for immunoblotting were from Santa Cruz Biotechnology Inc. Phosphorylation sites recognized by anti phosphor Ark1 and CaMKII antibodies are Ser473 and Thr286, respectively. For detection of phosphorylation of CnA, total protein (500 μg) of the LV tissue was immunoprecipated by an anti CnA antibody. The immunecomplexes were subjected to SDS-PAGE and blotted by an anti phosphor Ser antibody. The immunoreactivity was detected using an enhanced chemiluminescence reaction system (Amersham Pharmacia Biotech).

Detection of RyR-2 Protein Phosphorylation.

Cardiac SR was prepared from total LV lysates by centrifugation. [6] Total proteins from cardiac SR (200 μg) were incubated with an anti RyR-2 antibody (Santa Cruz Biotechnology Inc.) and the immunecomlexes were subjected to non-reducing gel electrophoresis. For RyR-2 phosphorylation with PKA, protein A sepharose beads were incubated with PKA catalytic subunit before gel fraction. [6] The membranes were immunoblotted with antibodies against RyR-2, FKBP12.6 or PKA (Santa Cruz Biotechnology Inc.).

p70 ^{S6} Kinase Activity

LV tissues were lysed with 0.15 mL of Triton X-100 lysis buffer (50 mmol/L Tris-HC1, pH 7.4, 100 mmol/L NaCI, 50 mmol/L NaF, 5 mmol/L EDTA, 40 mmol/L β-glycerophosphate, 1 mmol/L sodium orthovanadate, 0.1 mmol/L phenylmethylsulfonyl fluoride, 1 μmol/L leupeptin, 1 μmol/L pepstatin A, 1% Triton X-100) for 25 min on ice. Lysates (100 μg) were incubated for 12 hours at 4°C with anti-p70 ^{S6} kinase polyclonal antibody (Santa Cruz Biotechnology Inc.) preabsorbed to protein A-Sepharose beads. The immune complexes were washed 3 × with lysis buffer and once with kinase buffer (20 mmol/L N-2-hydroxyethylpiperazine-N'-2-ethanesulfonic acid (HEPES), pH 7.4, 10 mmol/L MgC12, 1 mmol/L dithiothreitol (DTT), 10 mmol/L β-glycerophosphate). The immunoprecipitates were resuspended in 40 μL of kinase buffer containing 0.2 mmol/L S6 peptide (RRRLSSLRA, Santa Cruz Biotechnology Inc.), 20 μmol/L ATP and 5 μCi of [γ-^{32}p]ATP (3000 Ci/mmol) and incubated at 30°C for 20 min. After incubation, the reactions were stopped by spotting the mixture on P81 paper (Whatman). The filters were washed 3 × for l0 min each in 1% phosphoric acid, once in acetone and dried. The ^{32}p uptake was measured by Cerenkov counting method. [7]

RT-PCR Analysis
Total RNA was isolated from LV tissues using TRIzol reagent (Gibco BRL). The expression of *GATA4* and *MEF2C* at the mRNA levels was evaluated using RT-PCR. The primers were as follows (forward/reverse): *GATA4*, gggccctctttgtcattcttc / tccttgctttctgcctgctac; *MEF2C*, gatgaagtgaagcgtggaagg/ cacagctcagttcccaaatcc. The PCR products were subject to electrophoresis on 1.5% agarose gels, scanned, and semi-quantitated using Image-Quant software (Kodak 1D V3.53; Kodak, New Haven).

HDAC Activity Analysis
Nuclear extracts of LV tissue were obtained with a Nuclear Extraction Kit (Bio Vision). Nuclear extract was then analyzed for HDAC activity with a HDAC Colorimetric Activity Assay Kit (Bio Vision, K331-100) according to manufacturer's instructions. The plate was read by a spectrophotometer at 400 nm absorbance and values were determined as O.D./μg protein in samples. [8]

Intracellular Ca^{2+} Levels by Ca^{2+} Fluorescent Dye Indo 1
Intracellular Ca^{2+} levels were measured with the Ca^{2+} fluorescent dye indo 1 (Dojin Kagaku). The ratio of 400-nm fluorescence to 500-nm fluorescence, which was collected from the cultured cardiomyocytes of neonatal rats illuminated by 360-nm light, was used as an indicator for intracellular Ca^{2+} concentration. [9]

CaMKII Activities
The activity of CaMKII was assayed by measuring the phosphorylation of synthetic peptide autocamtide-2, a peptide substrate for CaMKII. In brief, total proteins isolated from cultured cardiomyocytes were immunoprecipitated using an anti-CaMKII polyclonal antibody (Santa Cruz Biotechnology Inc.) and the immunecomplex was incubated with autocamtide-2 and [γ-^{32}P]ATP at the presence of Ca^{2+} and CaM. After incubation, the autocamtide-2 was collected using Whatman P81 paper and counted according to the Cerenkov's method. [9]

Calcineurin (CnA) Activities
The activity of CnA was determined with phosphorylated GST-RII peptide as a substrate. [9] We separated CaM-bound CnA (active CnA > 100 kDa) from free CnA (inactive CnA < 100 kDa) using Ultrafree-MC centrifugal filter units (Millipore).

Statistical Analysis
All values are expressed as mean ± S.D. of more than three experiments. Comparison between two groups was analyzed by the two-tailed, unpaired Student's *t*-test (normality) or non-parametric test (non-normality, Mann-Whitney *U*-test). We used Kolmogorov-Smirnov test for checking the normality. The normality was assumed by *P value* > 5. If *P value* < 5, the data weren't normal distribution, we used non-parametric test for analysis. Multiple group comparison was made by one-way ANOVA followed by Dunnetts' modified *t* test for comparison of means. Values of $P < 0.05$ were considered statistically significant.

Supplement Results

Upregulation of RyR-2 Phosphorylation by PKA in *RyR-2* Deficient Heart

At first, we confirmed that PKA phosphorylation completely dissociated FKBP12.6 from RyR-2 in WT mice (Figure 1, WT with PKA). The amount of FKBP12.6-associated RyR-2 was less in *RyR-2*$^{+/-}$ heart compared to WT heart, whereas PKA-phosphorylated RyR-2 in *RyR-2*$^{+/-}$ heart was more than WT one under basal conditions (Figure S1). TAC for 3 weeks decreased the amount of FKBP12.6-associated RyR-2 not only in WT mice but also in *RyR-2*$^{+/-}$ mice. TAC also increased the PKA-phosphorylated RyR-2 in both type of mice (Figure S1).

Affect of *RyR-2* Deficiency on TAC-induced *GATA2* and *MEF2C* Expression and HDACs Activity

There were no any significant differences in *GATA2* and *MEF2C* expression and HDACs activity between Sham-operated WT and *RyR-2*$^{+/-}$ mice (Figure S2). After TAC, the increases in *GATA4* mRNA expression in the heart of WT mice were significantly suppressed in *RyR-2*$^{+/-}$ mice, whereas the increase in *MEF2C* mRNA expression was not changed between the two types of mice. The increase in activity of HDAC in nuclear proteins in LV tissues after TAC for 3 weeks was not different between WT and *RyR-2*$^{+/-}$ mice. Our data suggest that CaMKII rather than calcineurin regulates activity of HDAC and transcription activation of MEF2C.

Downregulation of p70^{S6} Kinase Activity in the Heart of *RyR-2*$^{+/-}$ Mice after TAC

There was no significant difference in p70^{S6} kinase activity between Sham-operated WT and *RyR-2*$^{+/-}$ mice (Figure S3). The kinase activity was significantly elevated at 3 weeks after TAC in the heart of WT mice and the increase was suppressed in the heart of *RyR-2*$^{+/-}$ mice, consisting with the results of phosphorylation of Akt1.

Intracellular Ca^{2+} Levels and Activities of CaMKII and CnA

We used angiotensin II (AngII) as a stimulator for the intracellular Ca^{2+} levels and CaMKII and CnA activation since AngII is greatly involved in pressure overload-induced cardiac hypertrophy. AngII (10 nmol/L) could not induce increases in cytosolic free Ca^{2+} levels at both the systolic and diastolic phases in cultured cardiomyocytes of neonatal rats (Figure S4A). Although AngII rapidly (at 1 min) increased activities of CaMKII in a dose-dependent manner, it could not induce an increase in CnA activation (Figure S4B). These results suggest that CaMKII, but not CnA, could be activated without a global increase in Ca^{2+} levels in the cytoplasm.

References

1. Sano M, Minamino T, Toko H, Miyauchi H, Orimo M, Qin Y, Akazawa H, Tateno K, Kayama Y, Harada M, Shimizu I, Asahara T, Hamada H, Tomita S, Molkentin JD, Zou Y, Komuro I. p53-induced inhibition of Hif-1 causes cardiac dysfunction during pressure overload. *Nature.* 2007; 446:444-448.
2. Yao A, Su Z, Nonaka A, Nonaka A, Zubair I, Lu L, Philipson KD, Bridge JHB, Barry WH. Effects of overexpression of the Na^{+}-Ca^{2+} exchanger on $[Ca^{2+}]i$ transients in murine ventricular myocytes. *Circ Res.* 1998; 82:657-665.
3. Zou Y, Hiroi Y, Uozumi H, Takimoto E, Toko H, Zhu W, Kudoh S, Mizukami M, Shimoyama M, Shibasaki F, Nagai R, Yazaki Y, Komuro I. Calcineurin plays a critical role in the development of pressure overload-induced cardiac hypertrophy. *Circulation.* 2001; 104:97-101.
4. D'Souza KM, Malhotra R, Philip JL, Staron ML, Theccanat T, Jeevanandam V, Akhter SA. G protein-coupled receptor kinase-2 is a novel regulator of collagen synthesis in adult human cardiac fibroblasts. *J Biol Chem.* 2011; 286:15507-15516.
5. Zou Y, Komuro I, Yamazaki T, Kudoh S, Aikawa R, Zhu W, Shiojima I, Hiroi Y, Tobe K, Kadowaki T, Yazaki Y. Cell type-specific angiotensin II-evoked signal transduction pathways: critical roles of Gbetagamma subunit, Src family, and Ras in cardiac fibroblasts. *Circ Res.* 1998; 82:337-345.
6. Marx SO, Reiken S, Hisamatsu Y, Jayaraman T, Burkhoff D, Rosemblit N, Marks AR. PKA phosphorylation dissociates FKBP12.6 from the calcium release channel (ryanodine receptor): defective regulation in failing hearts. *Cell.* 2000; 101:365-376.
7. Takano H, Komuro I, Zou Y, Kudoh S, Yamazaki T, Yazaki Y. Activation of p70 S6 protein kinase is necessary for angiotensin II-induced hypertrophy in neonatal rat cardiac myocytes. *FEBS Lett.* 1996; 379:255-259.
8. Cardinale JP, Sriramula S, Pariaut R, Guggilam A, Mariappan N, Elks CM, Francis J. HDAC Inhibition Attenuates Inflammatory, Hypertrophic, and Hypertensive Responses in Spontaneously Hypertensive Rats. *Hypertension.* 2010; 56:437-444.
9. Zou Y, Yao A, Zhu W, Kudoh S, Hiroi Y, Shimoyama M, Uozumi H, Kohmoto O, Takahashi T, Shibasaki F, Nagai R, Yazaki Y, Komuro I. Isoproterenol activates extracellular signal-regulated protein kinases in cardiomyocytes through calcineurin. *Circulation.* 2001; 104:102-108.

Table S1. Ca^{2+} handling and contraction in adult cardiomyocytes.

Mice	WT			*RyR-2*$^{+/-}$		
TAC	-	+	*P*-value	-	+	*P*-value
Heart (n)	3	3	NS	3	3	NS
CM (n)	25	20	NS	28	20	NS
Ca^{2+} transient amplitude	1.15 ± 0.08	0.93 ± 0.04	< 0.05	0.5 ± 0.04*	0.3 ± 0.05‡	< 0.05
dCa^{2+}/dt of systolic phase	0.031 ± 0.004	0.024 ± 0.005	< 0.05	0.02 ± 0.003*	0.013 ± 0.001§	< 0.05
T1/2 of diastolic phase	349 ± 10	387 ± 17	< 0.05	363 ± 15	368 ± 10	< 0.05
FS%	5.0 ± 0.8	3.9 ± 0.7	< 0.05	3.3 ± 0.5†	2.5 ± 0.4§	< 0.05

Cardiac myocytes (CM) were isolated from adult male WT and *RyR-2*$^{+/-}$ mice with (+) or without (-) TAC for 3 weeks and intracellular Ca^{2+} concentration and contraction were analyzed. dCa^{2+}/dt of systolic indicates the rate of an increase in intracellular Ca^{2+} concentration; T1/2 of diastolic phase indicates the half-time of relaxation from caffeine-induced contracture; FS% indicates percentile fractional shortening of myocyte length. Data are shown as mean ± S.D. of 20~28 cardiomyocytes from 3 WT and 3 *RyR-2*$^{+/-}$ mice, respectively. * $P < 0.01$, † $P < 0.05$ *vs* WT mice without TAC; ‡ $P < 0.01$, § $P < 0.05$ *vs* WT mice with TAC. *P*-values indicate the comparison within the same genotype mice. NS, none statistically significant.

Table S2. Effects of Ryanodine on contraction of adult cardiomyocytes.

Mice	WT			*RyR-2*$^{+/-}$		
Ryanodine	-	+	*P*-value	-	+	*P*-value
Heart (n)	3	3	NS	18	18	NS
CM (n)	5.2 ± 0.7	2.8 ± 0.4	< 0.01	3	3	NS
FS %	20	20	NS	3.5 ± 0.8	2.5 ± 0.5	NS

Cardiac myocytes (CM) were isolated from adult male WT and *RyR-2*$^{+/-}$ mice. Percentile fractional shortening of myocyte length (FS%) was measured at the absent (-) or presence (+) of 100 μmol/L Ryanodine during electrical stimulation. Data are shown as mean ± S.D. of 18 and 20 cardiomyocytes from 3 WT and 3 *RyR-2*$^{+/-}$ mice, respectively. *P*-values indicate the comparison within the same genotype mice. NS, none statistically significant.

Figure S1

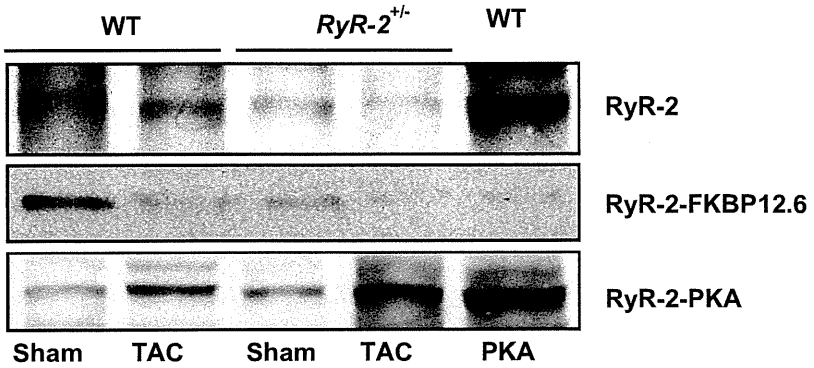

Figure S1. Association of FKBP12.6 and PKA with RyR-2. WT and *RyR-2*$^{+/-}$ mice were subjected to Sham or TAC for 3 weeks. Association of RyR-2 with FKBP12.6 and PKA was examined by western blot analyses for FKBP12.6 and PKA after immunoprecipated with an anti RyR-2 antibody. Phosphorylation of RyR-2 from WT mice with PKA (WT and PKA) was performed as described in Methods. Representative blots from 3 independent experiments are shown.

Figure S2

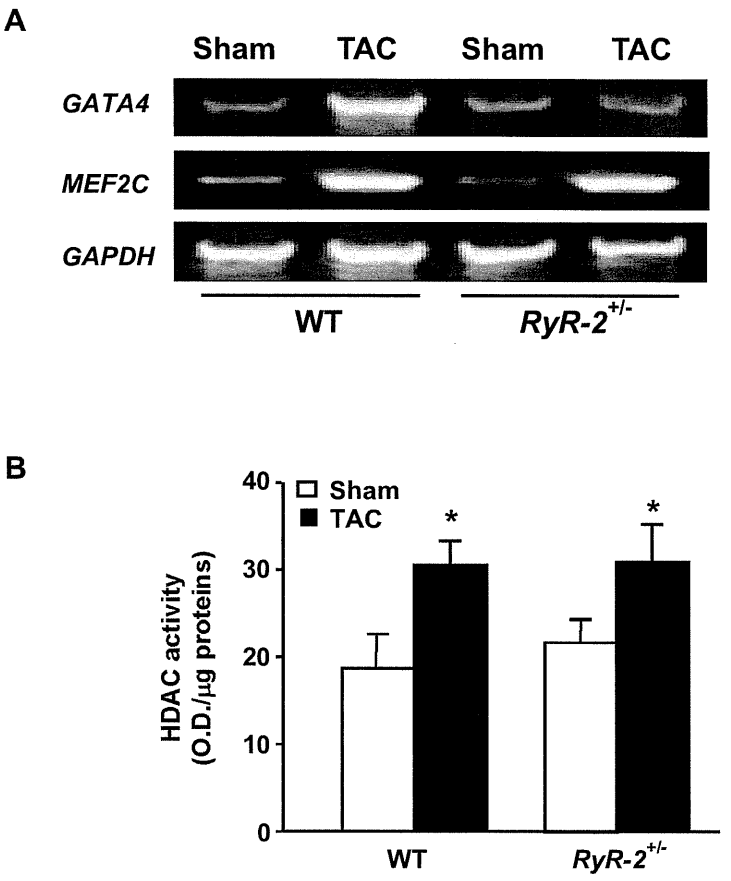

Figure S2. Expression of *GATA4* and *MEF2C* genes and activity of HDACs. WT and *RyR-2*$^{+/-}$ mice were subjected to Sham or TAC for 3 weeks. **A**. Expression of *GATA4* and *MEF2C* genes analyzed by RT-PCR. Representative photographs form 5 independent experiments are shown. **B**, HDAC activities. Data are expressed as mean ± S.D. from 5 hearts. * $P < 0.05$ *vs* sham-operated mice of the same genotype.

Figure S3

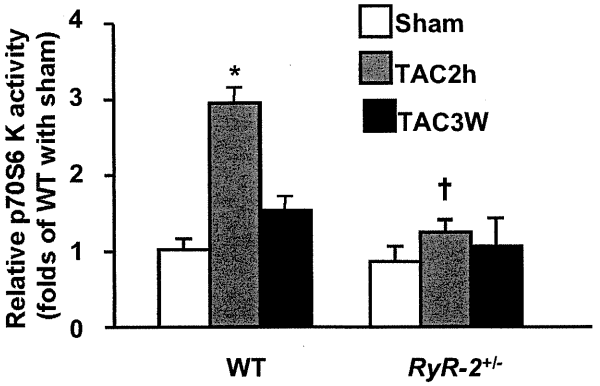

Figure S3. Activity of p70S6 kinase. WT and *RyR-2*$^{+/-}$ mice were subjected to Sham or TAC for 2 hours (2h) and 3 weeks (3W). p70S6 kinase activity was measured as described in Methods. Data are expressed as mean ± S.D. from 5 hearts. * $P < 0.05$ *vs* sham-operated mice of the same genotype; † $P < 0.05$ *vs* respective WT-TAC group.

Figure S4

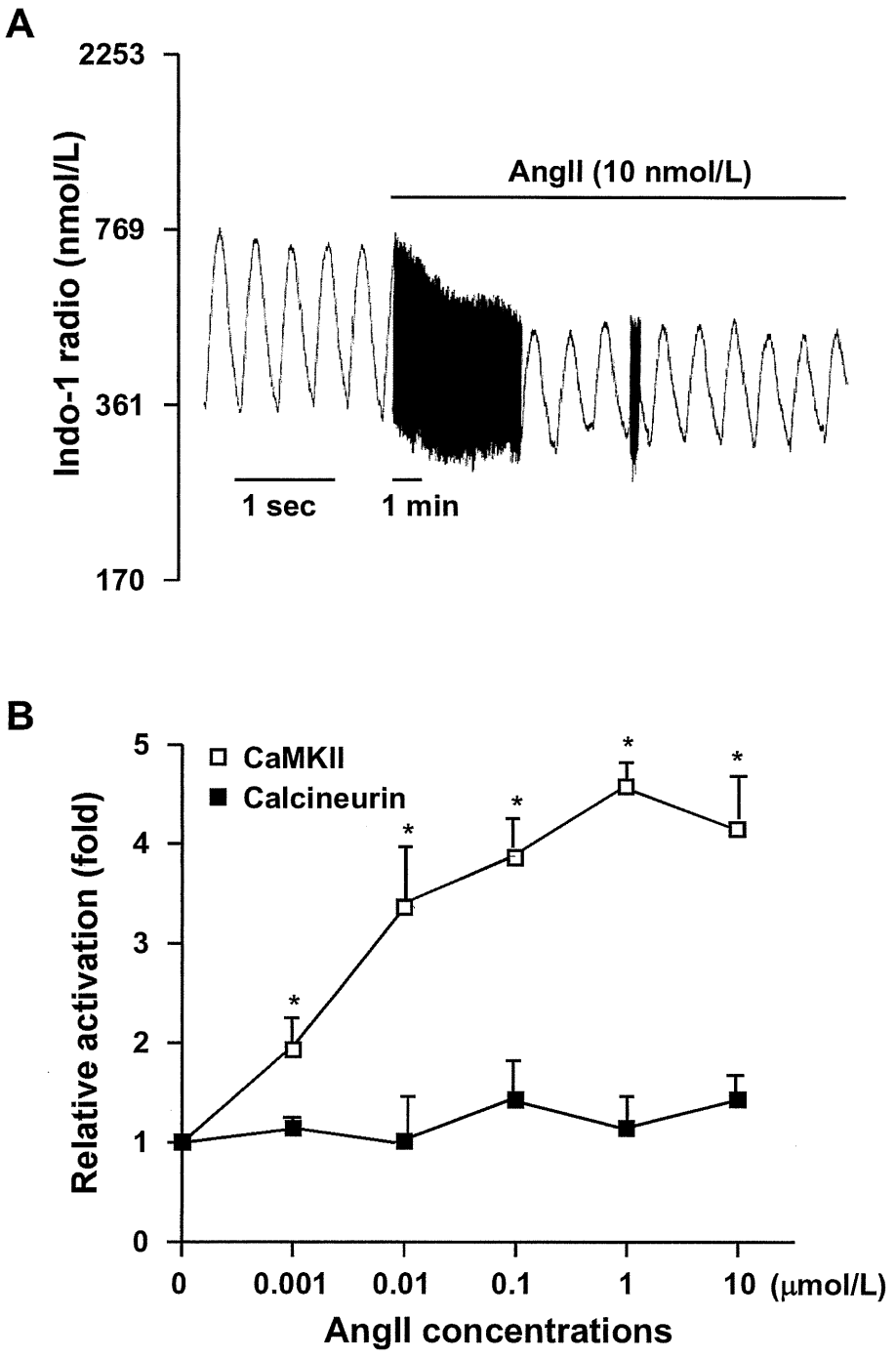
A
2253
769
361
170
Indo-1 radio (nmol/L)
AngII (10 nmol/L)
1 sec
1 min
B
CaMKII
Calcineurin
Relative activation (fold)
0
1
2
3
4
5
*
0
0.001
0.01
0.1
1
10 (μmol/L)
AngII concentrations

Figure 4. A, AngII-induced changes in intracellular Ca^{2+} levels in cardiomyocytes. Intracellular Ca^{2+} concentration was measured with fluorescent dye indo 1. Representative tracing of intracellular Ca^{2+} concentration transients before and after addition of AngII (10 nmol/L) is shown. **B**, Activation of CaMKII and CnA by AngII in cardiomyocytes. Cardiomyocytes were incubated with AngII at indicated concentration for 5 min. CaMKII and CnA activities were determined as described in Methods. Data represent mean ± S.D. from 3 independent experiments. $^{*}P < 0.05$ *vs* control.

OPEN ACCESS Freely available online

PLoS one

A Crucial Role of Activin A-Mediated Growth Hormone Suppression in Mouse and Human Heart Failure

Noritoshi Fukushima[1,2☯], Katsuhisa Matsuura[1,3*☯], Hiroshi Akazawa[4☯], Atsushi Honda[1], Toshio Nagai[5], Toshinao Takahashi[5], Akiko Seki[1], Kagari M. Murasaki[1], Tatsuya Shimizu[3], Teruo Okano[3], Nobuhisa Hagiwara[1,2], Issei Komuro[4*]

1 Department of Cardiology, Tokyo Women's Medical University, Tokyo, Japan, **2** Global Centers of Excellence (GCOE) Program, Tokyo Women's Medical University, Tokyo, Japan, **3** Institute of Advanced Biomedical Engineering and Science, Tokyo Women's Medical University, Tokyo, Japan, **4** Department of Cardiovascular Medicine, Osaka University Graduate School of Medicine, Osaka, Japan, **5** Department of Cardiovascular Science and Medicine, Chiba University Graduate School of Medicine, Chiba, Japan

Abstract

Infusion of bone marrow-derived mononuclear cells (BMMNC) has been reported to ameliorate cardiac dysfunction after acute myocardial infarction. In this study, we investigated whether infusion of BMMNC is also effective for non-ischemic heart failure model mice and the underlying mechanisms. Intravenous infusion of BMMNC showed transient cardioprotective effects on animal models with dilated cardiomyopathy (DCM) without their engraftment in heart, suggesting that BMMNC infusion improves cardiac function *via* humoral factors rather than their differentiation into cardiomyocytes. Using conditioned media from sorted BMMNC, we found that the cardioprotective effects were mediated by growth hormone (GH) secreted from myeloid (Gr-1(+)) cells and the effects was partially mediated by signal transducer and activator of transcription 3 in cardiomyocytes. On the other hand, the GH expression in Gr-1(+) cells was significantly downregulated in DCM mice compared with that in healthy control, suggesting that the environmental cue in heart failure might suppress the Gr-1(+) cells function. Activin A was upregulated in the serum of DCM models and induced downregulation of GH levels in Gr-1(+) cells and serum. Furthermore, humoral factors upregulated in heart failure including angiotensin II upregulated activin A in peripheral blood mononuclear cells (PBMNC) via activation of NFκB. Similarly, serum activin A levels were also significantly higher in DCM patients with heart failure than in healthy subjects and the GH levels in conditioned medium from PBMNC of DCM patients were lower than that in healthy subjects. Inhibition of activin A increased serum GH levels and improved cardiac function of DCM model mice. These results suggest that activin A causes heart failure by suppressing GH activity and that inhibition of activin A might become a novel strategy for the treatment of heart failure.

Citation: Fukushima N, Matsuura K, Akazawa H, Honda A, Nagai T, et al. (2011) A Crucial Role of Activin A-Mediated Growth Hormone Suppression in Mouse and Human Heart Failure. PLoS ONE 6(12): e27901. doi:10.1371/journal.pone.0027901

Editor: Piero Anversa, Brigham and Women's Hospital, United States of America

Received August 21, 2011; **Accepted** October 27, 2011; **Published** December 28, 2011

Funding: This study was supported by: The Global Centers of Excellence (COE) Program, Multidisciplinary Education and Research Center for Regenerative Medicine (MERCREM), from the Japanese Ministry of Education, Culture, Sports, Science and Technology (to N. Fukushima); a Grant-in-Aid for Scientific Research, Developmental Scientific Research, and Scientific Research from the Japanese Ministry of Education, Culture, Sports, Science and Technology; Uehara Memorial Research Grant (to KM); Grants from the Japanese Ministry of Education, Culture, Sports, Science and Culture and Health and Labor Sciences Research Grants (to HA); and a Grant-in-Aid for Scientific Research on Priority Areas and for Exploratory Research from the Japanese Ministry of Education, Culture, Sports, Science and Technology (to IK). The funders had no role in study design, data collection and analysis, decision to publish, or preparation of the manuscript.

Competing Interests: The authors have declared that no competing interests exist.

* E-mail: kmatsuura@abmes.twmu.ac.jp (KM); komuro-tky@umin.ac.jp (IK)

☯ These authors contributed equally to this work.

Introduction

Heart failure is a major cause of mortality in many countries. Infusion of bone marrow-derived mononuclear cells (BMMNC) is expected as a novel treatment of heart failure. Animal experiments and clinical trials have shown that BMMNC infusion ameliorates cardiac dysfunction after acute myocardial infarction and chronic myocardial ischemia [1]–[4]. Although the outcomes vary among trials, recent meta-analyses revealed that cardiac function slightly improves following BMMNC infusion for ischemic heart diseases [5], [6]. Bone marrow cells were reported to be incorporated into the damaged myocardium and to differentiate into various cell types including cardiomyocytes [7]. However, whether bone marrow-derived stem cells can differentiate into many cardiomyocytes is still an open question [8]. There are many reports indicating that transplantation of various types of stem cells improves the cardiac function of ischemic hearts, mainly by paracrine factors which induce angiogenesis and cardioprotection [9]–[11]. Since the effects of BMMNC infusion for non-ischemic cardiomyopathy remain unknown, we examined whether BMMNC infusion also improves cardiac function of non-ischemic cardiomyopathy.

Results

Preparation of non-ischemic dilated cardiomyopathy (DCM) mice

Two kinds of non-ischemic DCM mice were used. The first model was generated by transgenic overexpression of a mutant epidermal growth factor receptor (EGFR) with C-terminal truncation (EGFRdn). The expression of mutant EGFRdn is

activated by the cardiomyocyte-specific α-myosin heavy chain (αMHC) promoter (Figure 1A, Figure S1). EGFRdn mice exhibited heart failure and died at 5–30 weeks of age (Figure 1B). Gross inspection of the EGFRdn hearts showed global chamber dilatation with marked wall thinning (Figure 1C). The heart/body weight ratio was approximately 1.5-fold higher at 6 weeks of age in EGFRdn mice than in wild-type mice (Figure 1D). Echocardiography showed a significant decrease in the fractional shortening (FS) together with chamber dilatation (Figure 1E). In the second model, cardiomyopathy was induced by intraperitoneal injection of doxorubicin in wild-type mice. Doxorubicin-induced cardiomyopathy (DOX) mice showed marked dilatations of the left ventricular diastolic and systolic dimensions, and reduction of cardiac function (Figure S2).

Intravenous infusion of BMMNC transiently improved the cardiac function in DCM mice

BMMNC (2.0×10^7 cells) were isolated from wild-type healthy mice and intravenously infused *via* the tail veins to 8-week-old EGFRdn mice and 11-week-old DOX mice. An equal volume of PBS was infused into control mice. Three days after infusion, echocardiography showed that the FS was significantly improved in BMMNC-treated EGFRdn (Figure 2A) and DOX (Figure 2A) mice, compared with the respective controls. However, these effects were lost by 14 d after infusion (Figure 2A). When the infusion was repeated every 2 weeks, cardiac function showed improvements for >50 d (Figure 2B).

Although infusion of BMMNC is not promising for the treatment of heart failure, we may be able to apply alternative treatment if we understand the underlying mechanisms of beneficial effects of BMNNC infusion. To elucidate the mechanisms, we infused BMMNC derived from GFP mice. Although many GFP-positive cells were observed in the peripheral blood and the spleen at 3 d after infusion (Figure 2C, D), none were found in the heart, lung, liver, kidney or skeletal muscle (Figure 2E). At day 14, few GFP-positive cells were observed even in the peripheral blood (Figure 2C). This was consistent with the observation that BMMNC infusion improved cardiac function at day 3, but not at day 14. These results suggest that BMMNC infusion improves the systolic function of DCM mice not by transdifferentiation of BMMNC into cardiomyocytes but probably by humoral factors secreted from BMMNC. Size of each cardiomyocyte was larger in BMMNC-infused EGFRdn mice than in PBS-infused EGFRdn mice when infusions were repeated every 2 weeks for 8 weeks (i.e.,

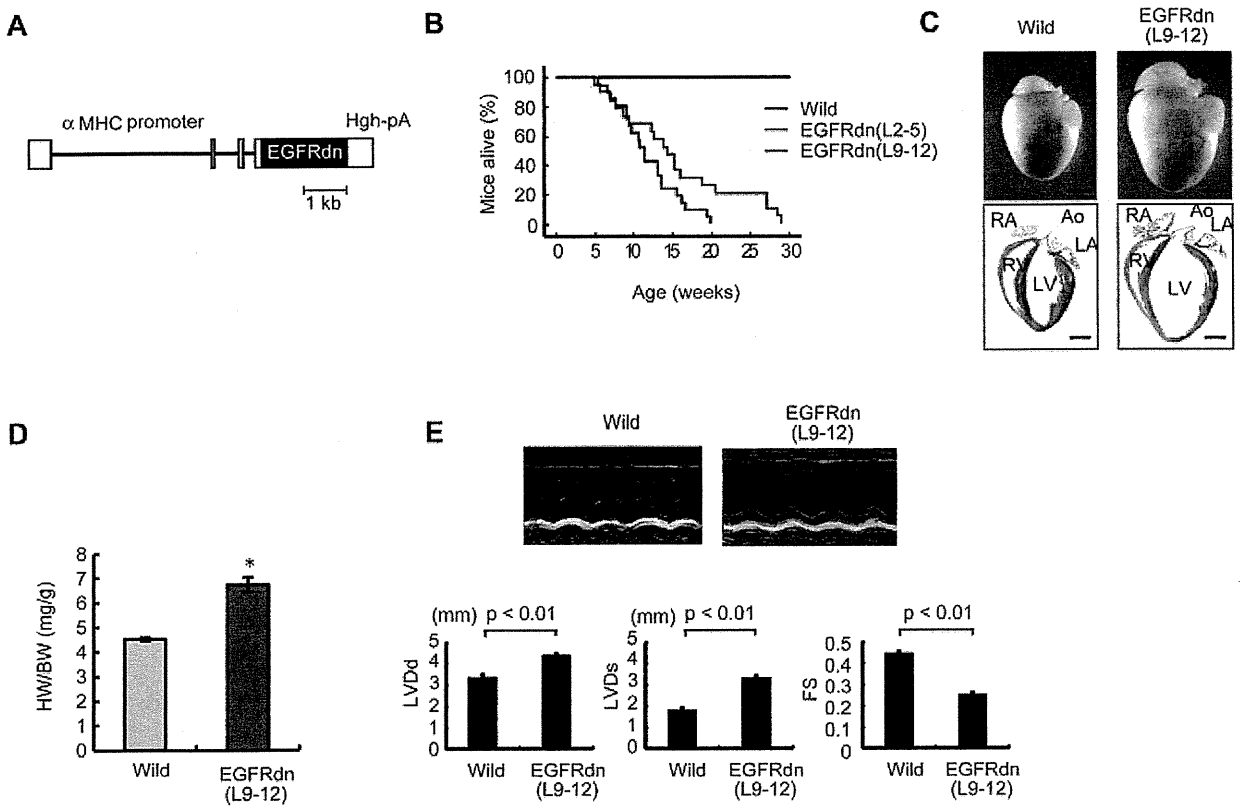

Figure 1. Transgenic overexpression of EGFRdn in the heart causes progressive heart failure. (A) Schematic representation of the cDNA construct used to generate EGFRdn mice. The construct contains an αMHC promoter, human EGFRdn cDNA and a human *growth hormone* polyadenylation signal (Hgh-pA). (B) Kaplan-Meier survival curves for wild-type ($n=62$) and EGFRdn (L2–5, $n=19$; L9–12, $n=21$) mice, showing a significant reduction in the survival rates in EGFRdn mice (log rank test, $P<0.0001$). (C) Gross morphology of whole hearts (upper panels) and longitudinal sections (lower panels) of hearts from wild-type and EGFRdn mice (L9–12) at 6 weeks of age. Ao, aorta; LA, left atrium; LV, left ventricle; RA, right atrium; RV, right ventricle. Scale bars: 2 mm. (D) Heart-to-body weight ratios (HW/BW) of wild-type ($n=9$) and EGFRdn (L9–12, $n=7$) mice at 6 weeks of age. *$P<0.01$. (E) Echocardiographic analysis. The upper photographs show representative M-mode images. The lower graphs show the left ventricular diastolic and systolic dimensions and FS of 8 week-old EGFRdn mice (L9–12) ($n=23$) and age-matched wild-type mice ($n=10$). LVDd, left ventricular diastolic dimension; LVDs, left ventricular systolic dimension. Data are means ± s.e.m.
doi:10.1371/journal.pone.0027901.g001

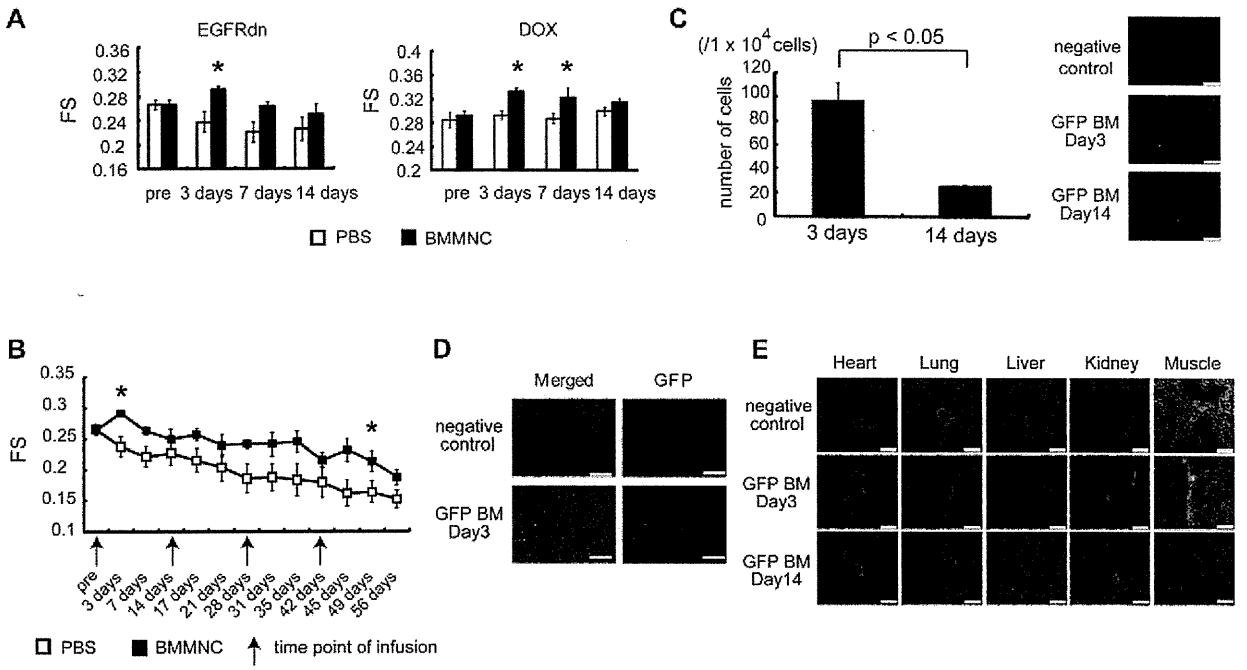

Figure 2. BMMNC infusion transiently improved the cardiac function of DCM mice. (A) Echocardiographic analysis. Transient improvements of FS were observed at 3 d in the BMMNC-treated group, but not the control (PBS) group, in EGFRdn mice (left), and at 3 and 7 d in DOX-treated mice (right). *$p<0.05$ versus PBS ($n=8$ per group). (B) Repeated-infusion experiments. BMMNC were infused every 2 weeks. A similar pattern of improvement in FS was observed after each infusion. *$p<0.05$ versus PBS ($n=8$ per group). (C–E) Immunohistochemical analysis. (C) Left, the number of GFP-positive BMMNC in peripheral blood ($n=3$). Right, photomicrographs of peripheral blood. Nuclei were stained with Hoechst 33258 (blue). Scale bars, 75 μm. (D) Images of the spleen 3 d after infusion. Many GFP-positive cells were observed in the spleen (lower photographs). Upper photographs, negative control. Nuclei were stained with Hoechst (blue color). Scale bars, 25 μm. (E) No GFP-positive cells were observed in any organs. Upper photographs, negative control. Middle and lower photographs, images taken at 3 and 14 d, respectively, after infusion. The vessels were stained with smooth muscle cell actin (red). Nuclei were stained with Hoechst 33258 (blue). The photographs of muscle are merged fluorescent and phase-contrast images. Scale bars, 75 μm. Data are means ± s.e.m.
doi:10.1371/journal.pone.0027901.g002

4 injections) (Figure S3). There were no changes in capillary density or the number of apoptotic cells in the heart between the BMMNC-infused group and the control group (data not shown).

BMMNC-derived conditioned medium (CM) improved cardiomyocyte contractility

To elucidate whether factors secreted from BMMNC were involved in their beneficial effects on cardiac function, we first examined the effects of CM from BMMNC on the contractility of cultured cardiomyocytes of neonatal rats. After serum starvation for 12 h, cardiomyocytes were challenged with culture medium conditioned by BMMNC. Cell shortening was significantly enhanced and beating rate was markedly increased at 30 min and at 12 h after starting culture with the CM, compared with those in untreated cells (Figure 3A), suggesting that BMMNC secrete factors that positively affect cardiomyocyte contractility. Flow cytometric analysis revealed that BMMNC consisted of several cell populations including myeloid (Gr-1(+) cells, ~40%), erythroid (TER119(+) cells, ~20%), and lymphoid cells (B220(+) cells, ~20%) (Figure S4). The individual cell populations, including the lineage-negative population of cells, were sorted by magnetic beads. The isolated cells were 0.8×10^7 Gr-1(+) cells, 0.4×10^7 B220(+) cells, 0.2×10^7 TER(+) cells, and 0.1×10^7 lineage-negative cells from 2.0×10^7 BMMNC. When CM was collected from each population and added to cardiomyocytes starved for 12 h, only the CM from Gr-1(+) cells significantly enhanced cell shortening and increased the beating rate (Figure 3B), suggesting that Gr-1(+) cells mainly contribute to BMMNC-mediated improvements in cardiomyocyte contractility. CM from Gr-1(+) cells or BMMNC isolated from wild-type mice also induced significant hypertrophy of cardiomyocytes (Figure S5). We next examined the effects of CM from Gr-1(+) cells on DOX mice. At 1 and 3 d after the infusion of CM from Gr-1(+) cells, FS was significantly improved, as with infusion of BMMNC (Figure 3C). Furthermore, +dp/dt, as determined by catheterization of the left ventricle, was also improved at 1 d after the infusion, as compared with the control group (Figure 3D). Collectively, these results indicate that factors secreted from Gr-1(+) cells are responsible for BMMNC-induced improvements in cardiac function in DCM mice.

Analysis of factors secreted from Gr-1(+) cells

The CM from wild-type Gr-1(+) cells significantly enhanced cell shortening and increased the beating rate, while CM from EGFRdn Gr-1(+) cells had marginal effects (Figure 4A). This suggests that the factors that improve cardiomyocyte contractility are more abundant in cells of wild-type mice than cells of EGFRdn mice. We next performed DNA microarray analysis to identify the factors involved in these effects. Twenty three genes showed enhanced expression in Gr-1(+) cells from wild-type mice compared with EGFRdn mice (Table 1). The gene which showed the largest difference between two types of mice was growth

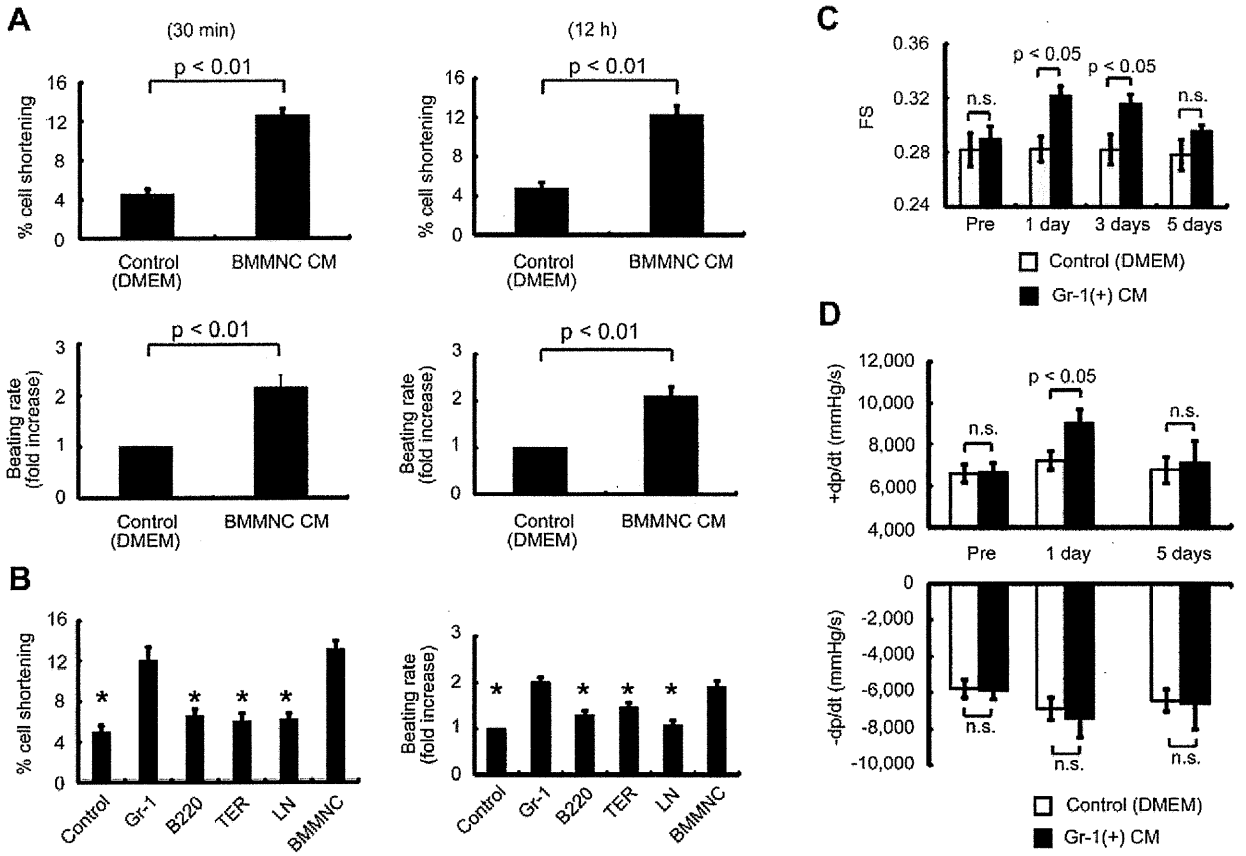

Figure 3. BMMNC-derived CM directly affects cardiomyocyte contractility. (A) Cell shortening and the beating rate of neonatal rat cardiomyocytes were significantly increased after exposure to CM from BMMNC compared with the control ($n = 26$ cells per group). The left and right graphs show the results at 30 min and at 12 h after treatment, respectively. Upper graph, cell shortening. Lower graph, beating rate. (B) CM from Gr-1(+) cells improved the cell shortening and increased the beating rate similar to that achieved by CM from BMMNC ($n = 27$ per group). (C, D) Effects of CM from Gr-1 cells on cardiac function *in vivo*. (C) Echocardiographic analysis ($n = 7$). The infusion of CM from Gr-1(+) cells significantly improved the FS of DOX mice at 1 and 3 d. (D) Infusion of CM from Gr-1(+) cells significantly improved the +dp/dt of DOX mice at 1 d, *in vivo* ($n = 7$). n.s., not significant. Data are means ± s.e.m.
doi:10.1371/journal.pone.0027901.g003

hormone (GH). The reduced expression of GH in Gr-1(+) cells from EGFRdn mice was confirmed by quantitative RT-PCR and ELISA (Figure 4B, C). GH levels were also lower in CM from Gr-1(+) cells isolated from old myocardial infarction (OMI) mice and DOX mice (Figure S6) than in CM from wild-type mice. Consistent with the downregulation of GH secretion from Gr-1(+) cells of heart failure mice, the serum GH levels were also lower in models of heart failure such as DOX, EGFRdn and OMI mice than in wild-type mice (Figure 4E).

Critical role of GH in Gr-1(+) cell-mediated cardioprotection

We examined the role of GH in the effects of Gr-1(+) cell-derived CM using pegvisomant, a specific inhibitor of the GH receptor [12]. Treatment with pegvisomant abolished the enhanced cell shortening and the increased beating rate induced by CM from Gr-1(+) cells (Figure 5A), while the anti-IGF-1 antibody had no effects (Figure 5B). These results suggest that Gr-1(+) cells improved the cardiomyocyte contractility *via* GH, but not *via* IGF-1 *in vitro*. CM from Gr-1(+) cells activated various signaling molecules, including Akt, extracellular signal-regulated kinase (Erk) 1/2, Janus kinase (Jak) 2, signal transducers and activators of transcription (Stat) 3/5 and protein kinase A (PKA) in cardiomyocytes (Figure 5C), and these effects were completely abolished by pegvisomant (Figure 5C). The addition of GH (500 pg/ml), a concentration equivalent to that in the CM from wild-type Gr-1(+) cells, activated the same signaling molecules (Figure 5C), suggesting that CM from Gr-1(+) cells activates Akt, Erk1/2, Jak2, Stat3/5 and PKA through the GH receptor signaling. Furthermore, the CM from Gr-1(+) cells, as well as GH, increased the amount of cyclic AMP (cAMP) in cardiomyocytes, which was also inhibited by pegvisomant (Figure 5D). The improvements in cardiac function induced by CM from Gr-1(+) cells were also abolished by treatment with the GH inhibitor (Figure 5E), whereas the anti-IGF-1 antibody had no effects (Figure 5F). Furthermore, the infusion of CM from Gr-1(+) cells increased the GH levels in serum of DCM mice (Figure 5G). These results suggest that Gr-1(+) cells improve the cardiac contractility *in vivo* also through GH. The BMMNC-mediated improvement in cardiac function of OMI mice was also affected by treatment with pegvisomant (Figure S7), suggesting that GH in BMMNC might have the therapeutic effects on heart failure caused by various etiologies.

Since Stat 3 is one of the important downstream targets of the GH receptor in cardiomyocytes (Figure 5C), we examined the

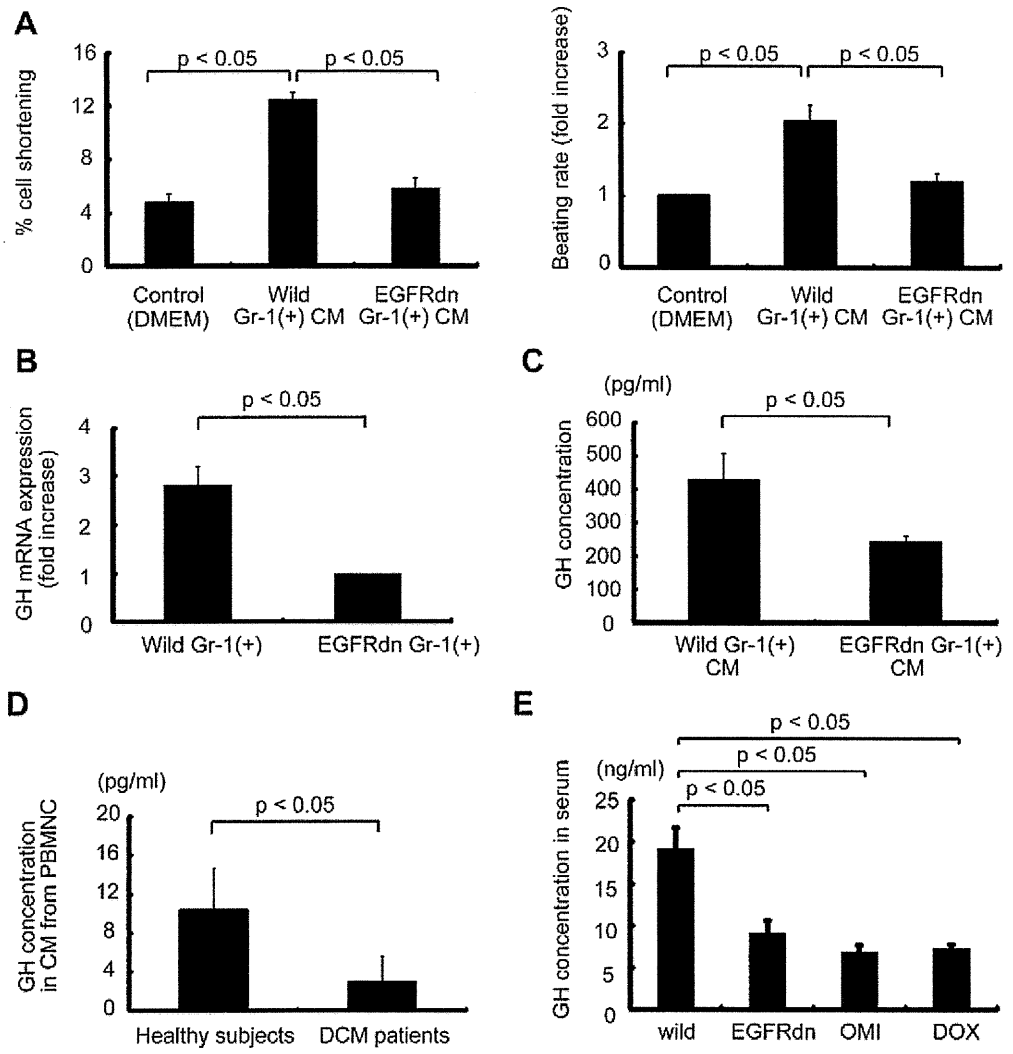

Figure 4. Analysis of secreted factors. (A) CM from Gr-1(+) cells from wild-type mice significantly improved the cell shortening and increased the beating rate in neonatal rat cardiomyocytes, as compared with CM from Gr-1(+) cells from EGFRdn mice. Left graph, cell shortening ($n = 24$ cells per group). Right graph, beating rate ($n = 24$ cells per group). (B) Quantitative RT-PCR analysis of GH mRNA in Gr-1(+) cells isolated from wild-type mice and EGFRdn mice ($n = 4$). (C, D) GH concentrations in (C) CM from Gr-1(+) cells isolated from wild-type mice and EGFRdn mice ($n = 4$) and (D) CM from PBMNC isolated from healthy ($n = 11$) and DCM subjects ($n = 10$). (E) GH concentration in serum from several mouse models of heart failure ($n = 4$). Data are means ± s.e.m.

doi:10.1371/journal.pone.0027901.g004

direct effects of GH in CM from Gr-1(+) cells on cardiomyocytes *in vivo* in transgenic mice overexpressing a dominant-negative mutant of STAT3 (STAT3dn) under the control of an αMHC promoter [13]. The Gr-1(+) cell CM-mediated improvements in cardiac function were not observed in DOX-treated STAT3dn mice (Figure S8), indicating that the CM improves cardiac function through activation of STAT3 in cardiomyocytes.

Upregulation of activin A in heart failure inhibits GH expression in Gr-1(+) cells

The expression of the GH gene has been reported to be regulated by transcription factors including pituitary transcription activator-1 (pit-1) [14], [15], and activin A has been reported to downregulate GH expression by reducing the stability of pit-1 [16]. Since activin A in the peripheral blood of heart failure patients has been reported to be upregulated compared with that in healthy controls [17], we investigated the role of activin A in the downregulation of GH in Gr-1(+) cells. Serum activin A levels were significantly higher in EGFRdn mice than in wild-type mice (Figure 6A), and were also elevated in other murine models of heart failure, including the OMI and DOX models (Figure S9). When Gr-1(+) cells were cultured with 400 pg/ml of activin A, a concentration equivalent to that in the peripheral blood of DCM mice, mRNA and protein levels of GH were significantly downregulated (Figure 6B), suggesting that activin A might be a key mediator of the reduced expression of GH in the Gr-1(+) cells of DCM mice. Furthermore, the serum activin A levels were remarkably higher in DCM patients (Table S1) than in healthy subjects (Figure 6A), while the GH levels in CM from peripheral blood mononuclear cells (PBMNC) of DCM patients was lower than that in healthy subjects (Figure 4D), suggesting that the

Table 1. DNA microarray analysis.

The fold increase	Gene symbol
4.9	Gh
4.3	Pdgfd
3.9	Figf
3.4	Tslp
3.2	Socs2
3.1	Lta
3.0	Bmp1
2.9	Il33
2.8	Ccl27a
2.7	Fgf20
2.6	Angpt1
2.5	Cxcl9
2.4	Il13
2.3	Fam3b
2.3	Il31
2.3	Gm6590
2.2	Spred1
2.2	Cmtm8
2.1	Kitl
2.1	Mif
2.1	Grem2
2.1	Il17d
2.1	Gdf10
2.0	Cxcl5

Each number indicates the fold-increase of gene expression in Gr-1(+) cells isolated from wild-type mice compared with those from EGFRdn mice.
doi:10.1371/journal.pone.0027901.t001

higher activin A levels might also inhibit GH expression in heart failure patients. A recent study showed that PBMNC are a major source of activin A in heart failure [17]. Since many humoral factors are known to contribute to the pathophysiology of heart failure [18], we examined whether humoral factors upregulated in heart failure might regulate activin A expression. Angiotensin II (AngII) (Figure 6C) and tissue necrosis factor-alpha (TNFα) (Figure S10A) increased the activin A levels in CM of PBMNC in a dose-dependent manner. Consistent with the previous reports [19], AngII and TNFα activated NFκB in the PBMNC (Figure 6D and Figure S10B) and AngII- and TNFα-induced upregulation of activin A in PBMNC were inhibited with a NFκB inhibitory peptide (Figure 6E and Figure S10C).

Inhibition of activin A in heart failure increases GH levels and improves cardiac function

To elucidate the role of activin A in EGFRdn mice, anti-activin A antibody was injected intraperitoneally for 2 weeks, with an alternate-day treatment regimen. Inhibition of activin A significantly increased GH protein levels in the CM from Gr-1(+) cells (Figure 6F). Furthermore, when neonatal rat cardiomyocytes were cultured with CM from Gr-1(+) cells isolated from anti-activin A antibody-treated EGFRdn mice, cell shortening was enhanced and the beating rate was increased significantly, as compared with CM from Gr-1(+) cells without antibody treatment (Figure 6G). Consistent with the upregulation of GH levels in Gr-1(+) cells by anti-activin A antibody treatment, the serum GH levels in EGFRdn mice were also increased (Figure 6H). Furthermore, FS and +dp/dt in EGFRdn mice treated with anti-activin A antibody were markedly improved compared with EGFRdn mice treated with isotype control (Figure 6H). Collectively, these results strongly suggest that inhibition of activin A improves cardiac function in non-ischemic DCM mice by restoring GH levels.

Discussion

Functional benefits of BMMNC infusion have been reported in human with ischemic heart diseases [2],[20]. Although we also observed the improvement of cardiac function of DCM model mice by BMMNC infusion, no engraftment of infused BMMNC was observed in the heart. At 3 d after infusion, BMMNC were only observed in the peripheral blood and spleen, but not in the heart, and very few GFP-positive cells were observed at 14 d even in the peripheral blood. This is consistent with the observations that BMMNC infusion only transiently improved cardiac function after infusion. These findings suggest that BMMNC improve cardiac function *via* humoral factors rather than *via* transdifferentiation into cardiomyocytes.

GH plays important roles in the protection of various tissues as well as the growth and development of many organs and whole body [21]. Serum GH levels have been reported to be low in patients with congestive heart failure [22]. Recent animal studies have demonstrated that GH treatment improves cardiac functions [23], [24]. The growth and protection of cardiomyocytes are regulated by various kinases such as Akt, Erk and Jak/Stat, and many studies have demonstrated that activation of Akt and Erk induces cardiac hypertrophy [25], [26] and prevents cardiomyocytes from stress-induced apoptosis [27]. Transgenic mice with cardiac-specific overexpression of the *stat3* gene were reported to show marked ventricular hypertrophy [28], while the cardioprotective effects of several cytokines including granulocyte colony-stimulating factor were reduced in mice with cardiac-specific expression of dominant-negative *stat3* [29]. In this study, we showed that GH produced by Gr-1(+) cells activated Akt, Erk, Jak2, Stat3/5 and PKA, and increased the levels of cAMP in neonatal rat cardiomyocytes (Figure 5C, D). GH has been reported to increase cAMP and activate PKA in reproductive organs by still-unknown mechanisms [30]. Here, we found that the beneficial effects of CM from Gr-1(+) cells on cardiac function were inhibited in cardiac-specific STAT3dn mice, suggesting that GH secreted by Gr-1(+) cells directly affects cardiomyocyte contractility. It has been reported that GH exerts some functions through the induction of IGF-1 expression [31], [32], and IGF-1 also promotes several cardioprotective effects in part by activating the Akt/phosphatidylinositol 3-kinase pathway [33], [34]. In the present study, the specific GH receptor inhibitor, but not anti-IGF-1 antibody, attenuated the improvements of cardiac contractility by the treatment of CM from Gr-1(+) cells in vitro (Figure 5A, B) and in vivo (Figure 5E, F). These findings suggest the effects of Gr-1(+) cells-derived CM on cardiac function of DCM mice mainly depend on GH rather than IGF-1.

It has been reported that the expression of GH gene is regulated by pit-1 at the transcriptional level [14], [15] and that activin A destabilizes pit-1 by phosphorylation [16]. Consistent with a previous report showing higher serum activin A levels in heart failure patients than in healthy controls [17], we found that serum levels of activin A were increased while GH levels in PBMNC CM were decreased in DCM patients. Similarly, the activin A levels were higher in the peripheral blood of DCM mice than in wild-type mice and activin A inhibited the production of GH in Gr-1(+)

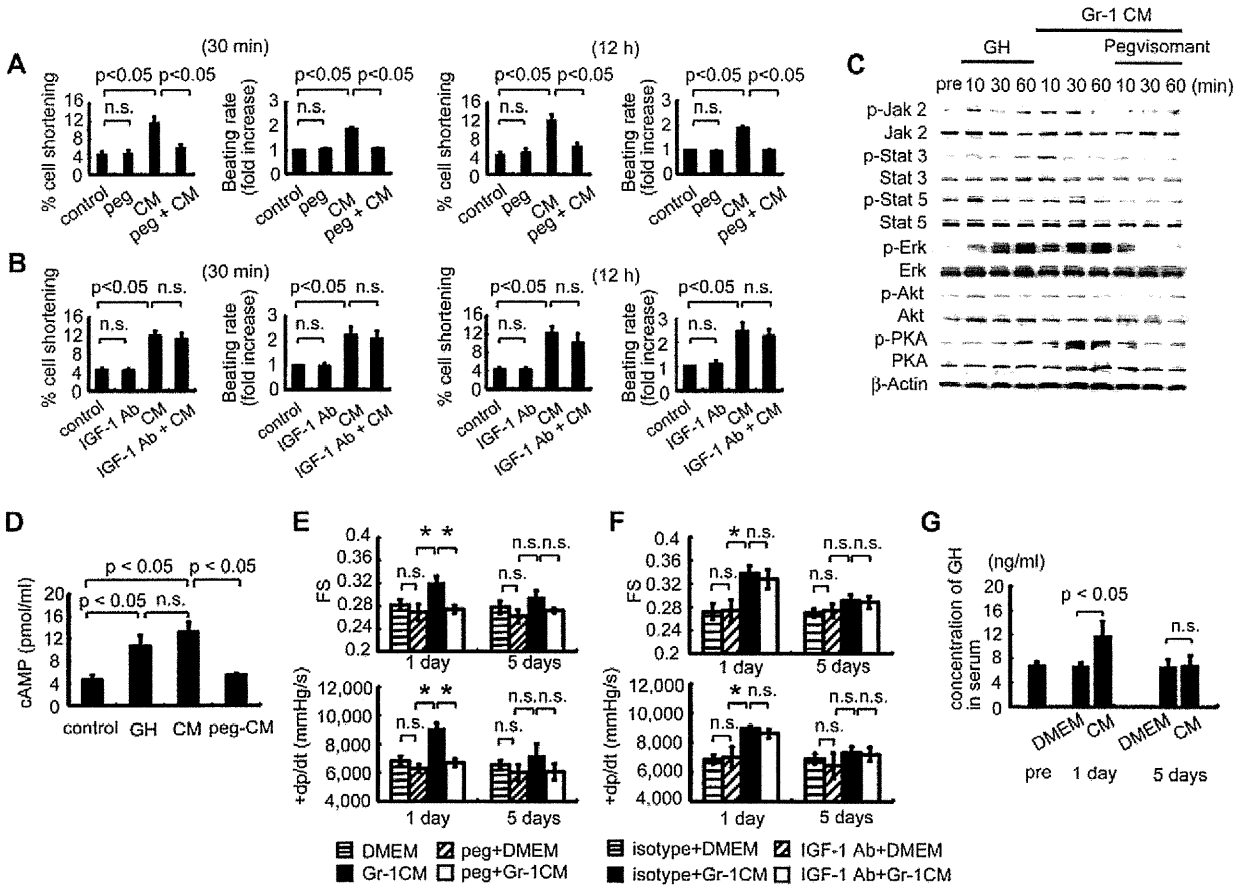

Figure 5. GH mediates the cardioprotective effects of Gr-1(+) cell-derived CM. (A) Pegvisomant (PEG) treatment inhibited the Gr-1(+) cell CM-mediated improvements cardiomyocyte cell shortening and beating rate at 30 min and at 12 h after treatment ($n=27$ cells per group). Left graphs, cell shortening; right graphs, beating rate. (B) Anti-IGF-1 antibody failed to affect the Gr-1(+) cell CM-mediated improvements in cell shortening or beating rate at 30 min or at 12 h after treatment ($n=23$ cells per group). Left graphs, cell shortening; right graphs, beating rate. (C) GH and CM from Gr-1(+) cells phosphorylated Akt, Erk, Jak2, Stat3/5 and PKA in cardiomyocytes ($n=3$), which was inhibited by pegvisomant ($n=3$). (D) GH (500 pg/ml) and CM from Gr-1(+) cells increased the cAMP concentration in cardiomyocytes ($n=5$), which was inhibited by pegvisomant ($n=5$). (E, F) Cardiac function analysis by echocardiography (upper graphs, $n=8$) and catheterization (lower graphs, $n=8$). Pegvisomant (E), but not anti-IGF-1 antibody (F), inhibited the improvements in FS and +dp/dt elicited by the infusion of CM from Gr-1(+) cells. *$p<0.05$ ($n=8$). (G) Serum GH concentrations in DOX mice treated with CM from Gr-1(+) cells ($n=4$ per group). The infusion of CM from Gr-1(+) cells from wild-type mice increased the serum GH concentration at 1 d, but not at 5 d. Data are means ± s.e.m.
doi:10.1371/journal.pone.0027901.g005

cells *in vitro*. These findings suggest that activin A, which is upregulated in heart failure, inhibits GH expression in various tissues/cells, including BMMNC. Treatment with anti-activin A antibody restored GH levels in Gr-1(+) cells and serum of EGFRdn mice and improved cardiac function, suggesting that normalizing the GH levels by inhibiting activin A is a novel therapeutic strategy for heart failure. Since many humoral factors such as AngII and TNFα are upregulated in heart failure and increased activin A expression by activating NFκB, the molecules that modulate NFκB activation might be also therapeutic targets to restore GH levels. On the other hand, anti-activin A treatment also increased expression levels of GH mRNA in the pituitary (N.F. K.M., unpublished data), suggesting that upregulation of activin A in heart failure might inhibit the expression of GH not only in Gr-1(+) cells but also in the pituitary, and that anti-activin A treatment might improve cardiac function of DCM mice in part by restoring GH expression in the pituitary.

The effects of GH on heart failure have been examined in many animal experiments and clinical trials [35]. A recent meta-analysis revealed that GH treatment improved several clinical parameters including left ventricular end-diastolic dimension, ejection fraction and New York Heart Association functional class [36]. Conversely, non-response to GH treatment for heart failure has been ascribed to GH resistance [37]. In patients with cardiac cachexia, GH levels were reported to be enhanced when compared with non-cachectic patients and normal subjects [38]. In this study, GH levels in heart failure mice and patients were significantly lower than those in healthy control subjects. Moreover, GH derived from Gr-1(+) cells improved cardiac function of heart failure animals, suggesting that our models were in a non-cachectic state and non-cachectic patients of heart failure might be suitable for GH treatment. Because of only temporary improvements in cardiac function (Figure 2A), bone marrow cell infusion might not be an appropriate treatment for heart failure, however inhibition

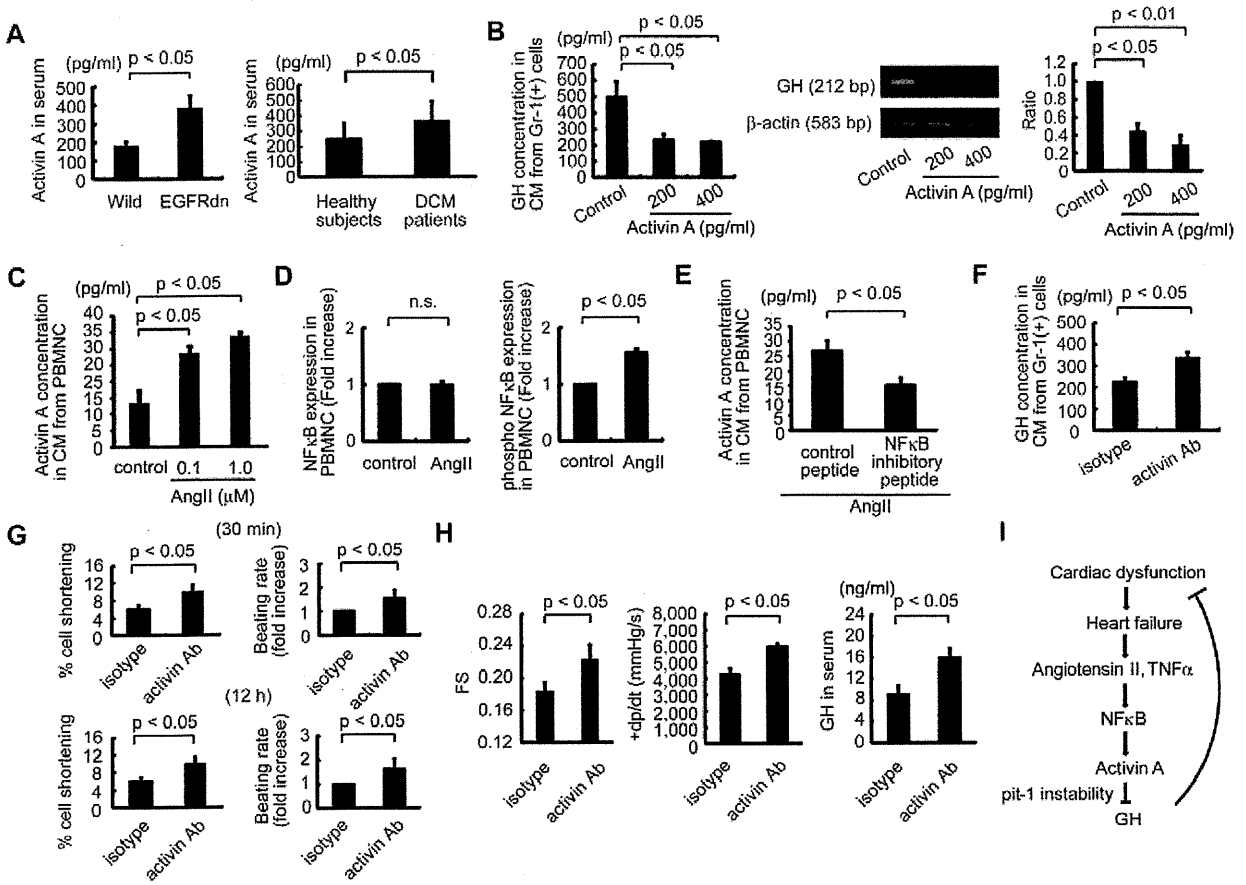

Figure 6. Regulatory mechanisms of GH in heart failure. (A) The serum activin A concentration was higher in EGFRdn mice (left, $n=5$) and in DCM patients (right, $n=10$) than in wild-type mice ($n=5$) and healthy subjects ($n=11$). (B) Activin A downregulated GH mRNA expression in Gr-1(+) cells and GH protein levels in Gr-1(+) cell CM. Left graph, GH protein concentration; middle photographs, representative semi-quantitative RT-PCR images; right graph, GH mRNA expression ($n=3$). (C, D) AngII upregulated activin A secretion (C, $n=4$) and phosphorylated NFκB expression (D, $n=5$) in wild-type PBMNC. (D) Left graph, total NFκB; right graph, phosphorylated NFκB. (E) Inhibition of NFκB [50 μM; NFκB p65 (Ser276) inhibitory peptide] suppressed AngII (10 μM)-mediated upregulation of activin A in CM derived from wild-type PBMNC ($n=5$). Isotype peptide was used as control. (F) The GH concentration in CM from EGFRdn Gr-1(+) cells ($n=5$) was significantly increased by treatment with an anti-activin A antibody ($n=5$). (G) Effects of anti-activin A antibody treatment on cell shortening and the beating rate of cardiomyocytes induced by CM from Gr-1(+) cells isolated from EGFRdn mice ($n=18$ cells per group). (H) Treatment with the anti-activin A antibody improved the cardiac function of EGFRdn mice. Left graph, echocardiography ($n=7$). Middle graph, miller catheter results ($n=7$). Right graph, serum GH concentration in EGFRdn mice after antibody treatment ($n=7$). Data are means ± s.e.m. (I) Proposed mechanism underlying impaired GH expression by activin A in heart failure.
doi:10.1371/journal.pone.0027901.g006

of activin A and enhancement of GH levels might offer novel therapeutic strategies for heart failure.

We used EGFRdn for DCM model mice in this study. It has been reported that cardiac-specific mutant of *ErbB2*, a member of the EGFR/erbB family, shows a severe dilated cardiomyopathy in mice [39]. In the clinical setting, trastuzumab, an anti-cancer agent, is humanized monoclonal antibody that targets the extracellular domain of the human epidermal growth factor receptor 2 and the use of trastuzumab demonstrated an unexpectedly high incidence of both asymptomatic and symptomatic cardiomyopathy. EGFRdn is a compatible DCM model mouse, resembling the cardiotoxic effects observed in patients treated with trastuzumab [40], [41].

There is a limitation in this study. We examined the surface area of neonatal rat cardiomyocytes after the treatment with CM from Gr-1(+) cells or BMMNC as an index for cardiac hypertrophy. However, the surface area not only depends on cell volume, but also on the degree of adhesion and spreading on the culture dishes.

Materials and Methods

Ethics Statement. The ethical committee of Tokyo Women's Medical University reviewed and approved the study protocol (approval ID: 1795). The study was conducted in accordance with the Declaration of Helsinki. We obtained informed consent from the all patients and the all healthy subjects by written before inclusion in this study.

Animals. Wild-type mice (C57BL/6) were purchased from Japan SLC. Adult GFP transgenic mice (C57BL/6) were a kind gift from Dr. M. Okabe (Osaka University). Cardiac-specific dominant-negative STAT3 mice were a kind gift from Dr. K. Yamauchi-Takihara (Osaka University). Neonatal Wistar rats (0–1 d old) were purchased from Saitama Experimental Animals Supply. All protocols were approved by the Institutional Animal Care and Use Committee of Tokyo Women's Medical University and Chiba University. The approval IDs for the animal experiments were 11–34 in Tokyo Women's Medical University